Research paper

Aluminum powders: aging effects on metal content and thermogravimetry reactivity

Christian Paravan*†, Alberto Verga*, Stefano Dossi*, Filippo Maggi*, and Luciano Galfetti*

*Politecnico di Milano, Aerospace Science and Technology Department, Space Propulsion Laboratory (SPLab), 34, via LaMasa, 20156, Milan, ITALY
Phone: +39 0223998068
†Corresponding author: christian.paravan@polimi.it

Received: December 2, 2017 Accepted: September 14, 2018

Abstract

Nano-sized Al (nAl) features high reactivity implying possible issues related to its aging during storage. In this work, the aging behavior of micron-sized Al and nAl is investigated considering different relative humidity (RH) conditions (10% and 80%) at the temperature of 333 K. The marked aging sensitivity of nAl (100 nm) is testified by an almost full metal content (C_{Al}) loss in nearly 30 hours ($RH = 80\%$). Under the same condition, in 14 days of aging, the C_{Al} of micron-sized aluminum (30 μm) decreases from $(99.1 \pm 0.2)\%$ to $(86.8 \pm 0.9)\%$.

Keywords: nano-sized aluminum, micron-sized aluminum, aging, metal content, thermogravimetry reactivity

Nomenclature

D_{32}	surface-based mean particle diameter [nm]
$T_{end,i}$	i-th intense oxidation end temperature [K]
$T_{onset,i}$	i-th intense oxidation onset temperature [K]
$\alpha_{Al \rightarrow Al_2O_3}(T)$	Al → Al_2O_3 conversion factor, $\Delta m(T)/(C_{Al} \cdot 0.89)$ [%]
$\alpha_{Al \rightarrow Al(OH)_3}(t)$	Al → $Al(OH)_3$ conversion factor, $\Delta m(t)/(C_{Al} \cdot 1.889)$ [%]
Δm_0	mass change due to desorption/dehydration [%]
Δm_1	mass change in the first oxidation step [%]
Δm_{933K}	mass change at 933 K [%]
Δm_{1223K}	mass change at 1223 K [%]

1. Introduction

Aluminum is a high density energetic material widely used in solid propellants and fuels for rocket propulsion[1)–6)]. Currently, commercial solid propellants are based on air-passivated micron-sized aluminum (μAl) with size in the range 50–15 μm. These powders are characterized by metal contents (C_{Al}) typically higher than 95 wt%, and specific surface area (SSA) lower than 1 $m^2\ g^{-1}$. Nano-sized Al (nAl) features increased reactivity over the conventional μAl[1),4),6)]. In general, air-passivated nAl exhibits $SSA \geq 10\ m^2\ g^{-1}$, and $C_{Al} < 90$ wt%[1),6)]. While attractive in terms of the enhanced performance in a combustion environment, nAl high reactivity may yield issues related to aging under storage. Few open literature studies deal with the aging process of Al powders[7)–12)], while aging effects (under non-fully controlled/reported conditions) are observed in different publications.

This paper investigates the accelerated aging behavior of aluminum powders with various particle sizes. Tested powders range from conventional μAl to nAl. The collected data show the aging effects on powder energetic content (C_{Al}) and reactivity (evaluated by thermogravimetry, during slow heating rate oxidation).

2. Materials and experimental methods

2.1 Tested powders

Tested powders are commercially available, uncoated and passivated by air. Micron-sized powders (μAl-30, and μAl-7.5) are produced by AMG Alpoco (UK). The nAl powder (nAl-100) is produced by APT-Advanced Powder Technology LLC (Russia).

2.2 Powder characterization

Tested powders were characterized in terms of particle size distribution by Malvern Mastersizer 2000, using both dry and liquid dispersion units (for micron- and nano-sized

Table 1 Initial characteristics of the tested μAl and nAl powders. The *SSA* -based diameter is evaluated as $a_s = 6/(\rho_{Al} \cdot SSA)$, with $\rho_{Al} = 2700$ kg m^{-3}.

Id.	Nominal size [nm]	*SSA* [m^2 g^{-1}]	a_s [nm]	D_{32} [nm]	C_{Al} [wt%]
μAl-30	30000	< 0.1	> 22000	28900	99.1 ± 0.2
μAl-7.5	7500	< 0.1	> 22000	4150	95.3 ± 0.2
nAl-100	100	12.6 ± 0.1	176	133	85.7 ± 0.6

materials, respectively). The specific surface area was determined by N_2 adsorption/desorption isotherms and the BET equation[1]. The C_{Al} was evaluated by a volumetric method based on the Al+H_2O reaction[1),5),6)]. Thermogravimetry (TG) analyses were performed in air, with heating rate of 10 K min^{-1}. Powder reactivity was determined exploiting the parameters suggested by Ilyin et al.[13].

2.3 Aging conditions

The aging of the powders was studied under a temperature of 333 K, to accelerate the corruption process. Two different conditions of *RH* were considered to highlight the effects of the H_2O vapor concentration. In the dry environment D1 condition, $RH < 10\%$ (dry air + SiO_2), while in the humid environment H1 condition $RH = (80.2 \pm 0.4)\%$ (saturated H_2O + KCl solution). Accelerated aging conditions were produced in sealed glass containers with internal volume of 0.5 dm^3. These vessels were prepared and stored at $T = 333$ K for 24–48 hours, before the start of the experiments. Small amounts of powder (0.3–0.4 g) were inserted in glass weighting bottles with diameter of 30 mm. The (opened) weighting bottles were placed in small plastic jars and were then inserted in pre-prepared, sealed glass vessels containing the test environment. The reduced amount of powder granted a uniform exposure of the sample to the aging environment without any mixing.

3. Experimental results and discussion

Experimental results are hereby presented for the initial powder characterization and for the aging study. Thermal analysis data and C_{Al} results are presented as average of at least two and four different runs respectively. In both cases, intervals of confidence are reported in terms of standard deviation.

3.1 Initial characterization

The tested air-passivated powders are listed in the Table 1. Micron-sized powders show D_{32} values in agreement with the nominal size. The μAl-7.5 features $D_{32} = 4150$ nm, due to a bimodal distribution with a small powder fraction (< 3.0 vol.%) of sub-micrometric size (400 −1000 nm). The nAl-100 *SSA* -based particle diameter[13] (a_s) shows a general agreement with the D_{32} from laser granulometry. X-ray diffraction analyses performed on the fresh powders revealed metallic Al as the unique crystalline phase in the materials. Scanning and transmission electron microscopies of the tested powders are reported elsewhere[1]. TG traces for the non-isothermal oxidation of μAl-30, μAl-7.5 and nAl-100 are reported in the Figure 1. The reactivity parameters for the TG analyses are presented in the Table 2. The powder first oxidation onset is below the Al melting point (933 K), and is related to the amorphous to γ-Al_2O_3 phase transition[4]. The $T_{onset,1}$ shows no clear correlation with the powder size, as evidenced by the intense oxidation onset temperature for the nAl-100 with respect to the μAl-7.5. The finer micron-sized powder features a faint and slow oxidation process, in turn yielding an apparent onset reduction when applying the tangent method (see Figure 1(b)). The increased *SSA* of nAl-100 yields an increased reactivity over the μAl-counterparts, as testified by the Δm_{933K}, $\alpha_{Al \rightarrow Al_2O_3}$ (933 K) and $\alpha_{Al \rightarrow Al_2O_3}$ (1223 K) values. For both the micron- and the nano-sized particles, the metal core melting does not affect the powder reactivity under the tested TG conditions.

3.2 Aging effects

3.2.1 Dry environment (D1)

Tests performed under $RH < 10\%$ show a similar trend of the relevant parameters between μAl and nAl specimens (see Figure 2). The powder mass is nearly unchanged during a period of 14 days, independently from the powder dispersity. The relatively low H_2O content in the aging environment limits the corruption of the Al_2O_3 shell (i.e., its transformation into hydrated species as $Al(OH)_3$). Over the 14 days aging period, the C_{Al} of μAl-30 shows no decrease. Similarly, the active metal content of μAl-7.5 shows values of (94.8 ± 0.4)% at 7 days and (94.2 ± 0.6)% at 14 days, being substantially unchanged. Active metal content of nAl-100 after 14 days of storage at $RH < 10\%$ is (85.6 ± 0.3)%. TG analyses show that after dry environment storage, nAl-100 mass loss due to the adsorbed gas desorption is (−0.9 ± 0.1)%, while $T_{onset,1} = (857.5 \pm 0.1)$ K and the conversion factor from Al → Al_2O_3 at 933 K and 1223 K are (38.7 ± 0.2)% and (84.8 ± 0.6)% respectively.

3.2.2 Humid environment (H1)

For the H1 tests, the Al→$Al(OH)_3$ conversion factor $\alpha_{Al \rightarrow Al(OH)_3}(t) = \Delta m(t)/(C_{Al} \cdot 1.889)$ is defined as a function of the aging time (t). The $C_{Al}(t)$ and the $\alpha_{Al \rightarrow Al(OH)_3}(t)$ are shown in Figure 3 for μAl-30, μAl-7.5 and nAl-100. Note that the $\alpha_{Al \rightarrow Al(OH)_3}(t)$ reflects the mass increase behavior of the tested powders. The powder *SSA* shows an influence on the powder aging, as shown in Figure 3.

Micron-sized powders exhibit an initial decrease of the $C_{Al}(t)$. This is then followed by a stabilization of the metal content in time. The μAl-30 shows a C_{Al} change from

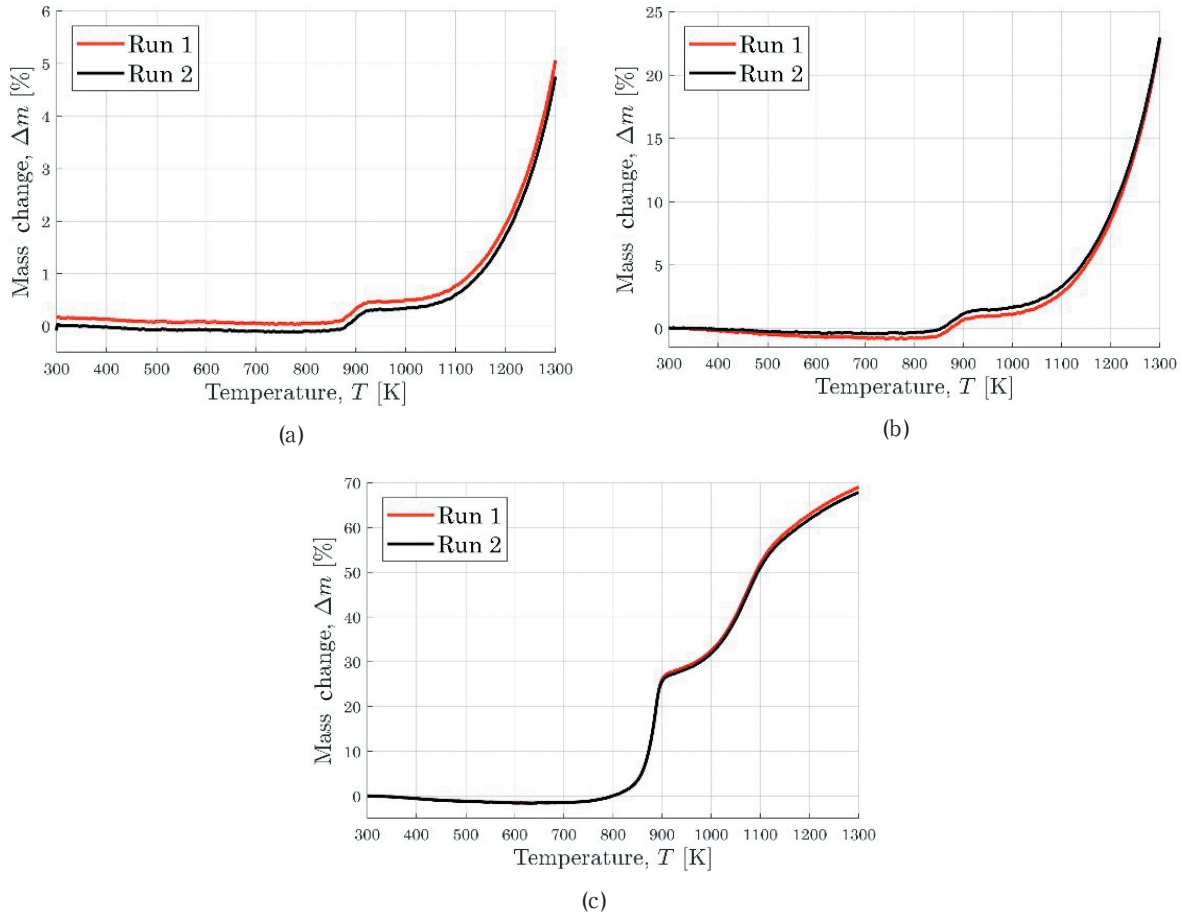

Figure 1 TG traces (air, 10 K min^{-1}, 0.1 MPa) of fresh (a) μAl-30, (b) μAl-7.5, and (c) nAl-100.

Table 2 Fresh Al powder reactivity parameters (TG, 10 K min^{-1}, air, 0.1 MPa).

	μAl-30	μAl-7.5	nAl-100
Δm_0 [%]	−0.2 ± 0.1	−0.6 ± 0.3	−1.6 ± 0.4
T (Δm_0)[K]	782.7 ± 2.1	741.2 ± 0.7	663.4 ± 1.9
$T_{onset,1}$[K]	865.0 ± 0.3	842.5 ± 0.5	856.1 ± 0.2
Δm_1, [%]	0.5 ± 0.1	1.8 ± 0.5	28.2 ± 0.4
$T_{end,1}$ [K]	915.3 ± 0.6	905.2 ± 0.4	898.4 ± 0.5
Δm_{933K}[%]	0.5 ± 0.2	1.8 ± 0.5	29.5 ± 0.4
$\alpha_{Al\rightarrow Al_2O_3}$ (933 K) [%]	0.6 ± 0.1	2.2 ± 0.6	38.7 ± 0.6
$T_{onset,2}$ [K]	1224.2 ± 0.4	1203.3 ± 0.4	1014.9 ± 0.5
$T_{end,2}$ [K]	NAv.	NAv.	NAv.
Δm_{1223K} [%]	2.5 ± 0.2	11.6 ± 0.5	65.6 ± 0.8
$\alpha_{Al\rightarrow Al_2O_3}$ (1223 K) [%]	2.9 ± 0.2	13.7 ± 0.5	86.0 ± 1.1

(99.1 ± 0.2)% to (86.8 ± 0.9)%, with a $\alpha_{Al\rightarrow Al(OH)_3}$ (14 days) = (4.7 ± 0.2)%. The μAl-7.5 shows a similar behavior, with C_{Al} (7 days) = (58.1 ± 0.8)%. This value is further decreased to (55.8 ± 0.6)% for t = 14 days. The $\alpha_{Al\rightarrow Al(OH)_3}$ (14 days) is (21.3 ± 1.4)%. The increased aging sensitivity of μAl-7.5 is likely due to the reduced particle size yielding increased reactivity over the coarser μAl-30 (Table 2 and Table 3). The nAl-100 is more prone to aging, due to the increased *SSA* (Figure 3(c)). A nearly complete corruption of the original C_{Al} is achieved in less than 30 hours. After 48 hours, the active metal content of the powder is (2.3 ± 0.3) %, and the corresponding $\alpha_{Al\rightarrow Al(OH)_3}$ is (96.3 ± 0.9)%. The mass gain during the powder aging in a wet environment is initially due to the adsorption of H_2O on the particle surfaces and the following formation of hydrated species as $Al(OH)_3$ and/or AlO(OH).

Table 3 reports the TG reactivity parameters for the aged powders. Micron-sized Al powders show a general increase of the $T_{onset,1}$ after aging. This is probably due to the initial corruption of the Al_2O_3 shell yielding Al+H_2O reaction, with the creation of hydrated species. These hydrated species feature a reduced passivation effect, thus yielding further C_{Al} decrease (in turn implying a thickened shell surrounding the residual metal core). Hydrated species are dehydrated during the TG heating[14], leaving a relatively thick Al_2O_3 layer that, in turn, reduces the powder reactivity at slow heating rates (see Figure 4). For nAl-100, no significant reactivity changes are identified for the earlier phases of the aging (Table 2 and Table 3). Passing to the aging times of 24 and 72 hours, the main observed phenomenon is the specimen mass loss (see Table 3). The Δm_0 agrees with the mass loss limit due to $Al(OH)_3$ dehydration to Al_2O_3, as reported by Sato[14]. For 72-hours aging, nAl-100 C_{Al} is nearly completely consumed, and a low conversion to Al_2O_3 is achieved due to the shielding action exerted by the refractory shell produced after the dehydration of the species formed during the aging.

4. Conclusions and future developments

This work focuses on the analysis of the effects of accelerated aging on the reactivity of micron- and nano-

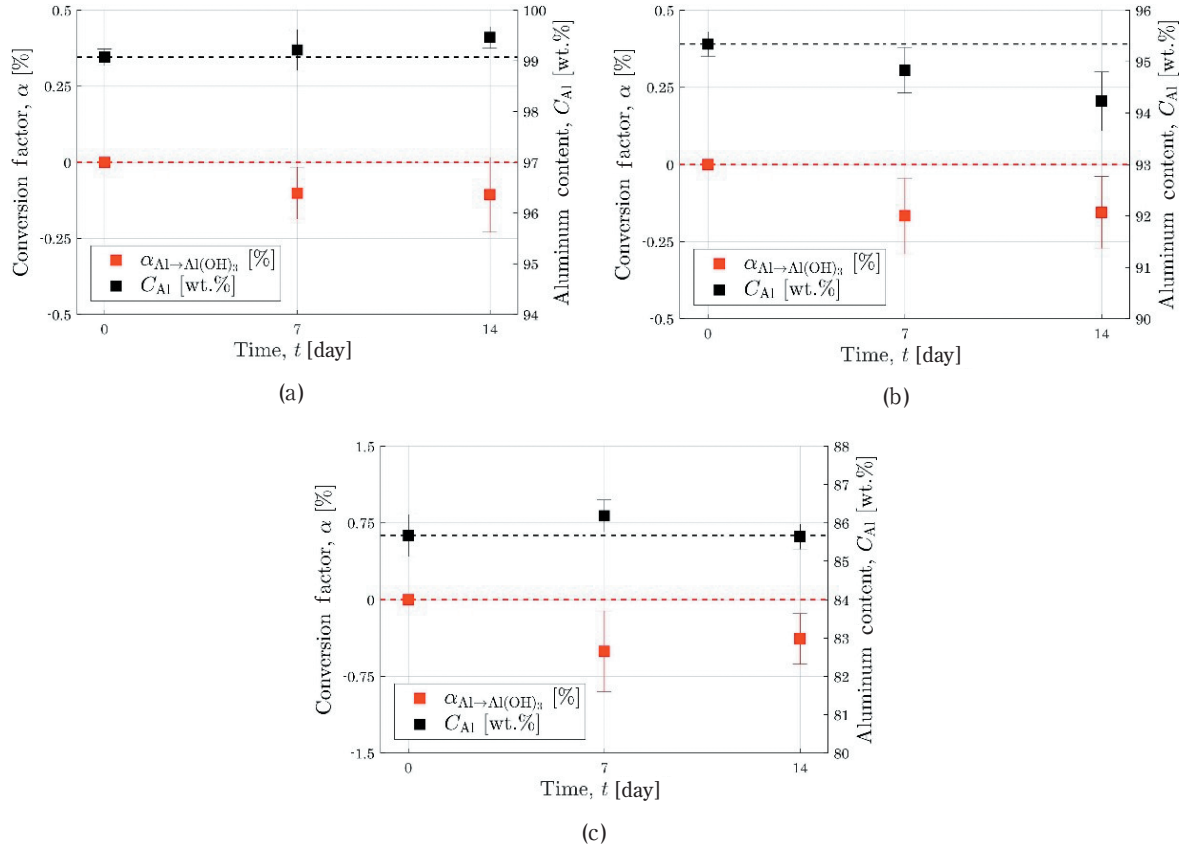

Figure 2 Accelerated aging: $C_{Al}(t)$ and $\alpha_{Al\rightarrow Al(OH)_3}(t)$ for (a) μAl-30, (b) μAl-7.5, and (c) nAl-100, all under D1 condition.

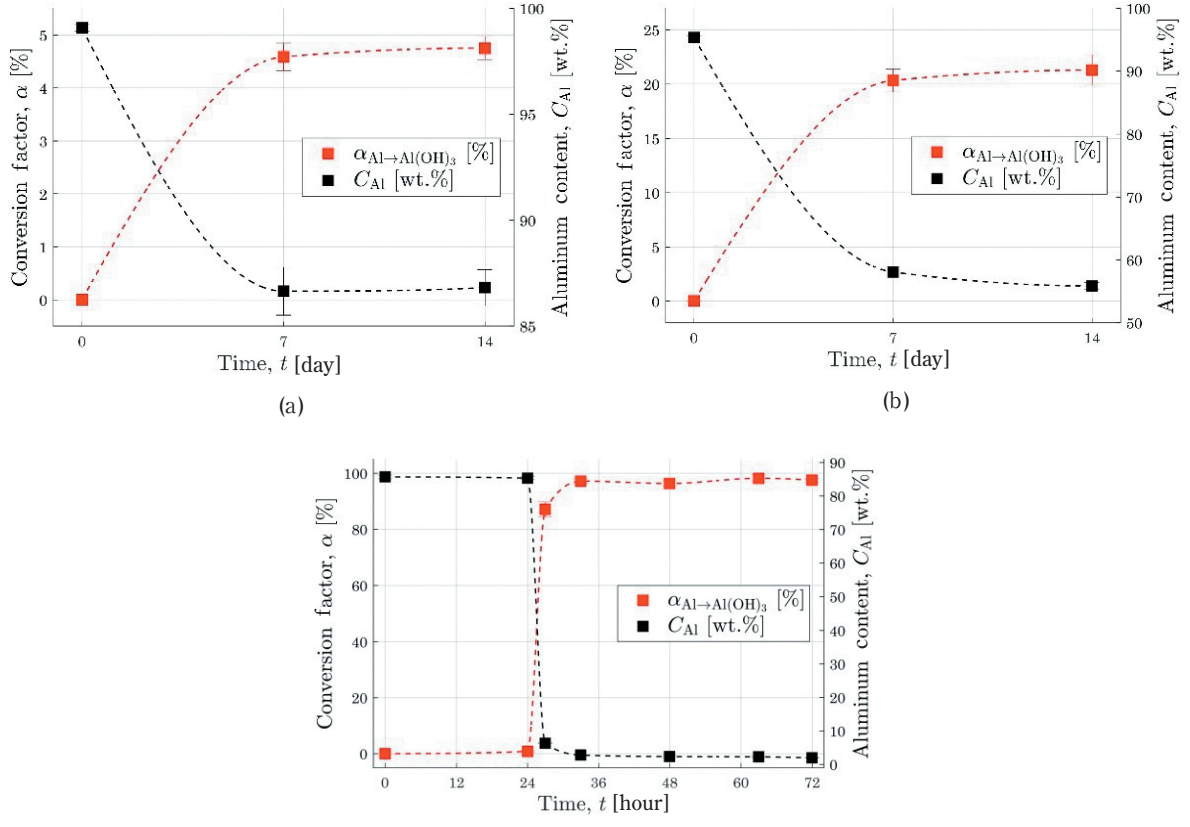

Figure 3 Accelerated aging: $C_{Al}(t)$ and $\alpha_{Al\rightarrow Al(OH)_3}(t)$ for (a) μAl-30, (b) μAl-7.5 and (c) nAl-100, all under H1 condition.

Table 3 Reactivity parameters for TG analyses (air, 10 K min^{-1}, 0.1 MPa) of tested Al powders during/after aging (H1 condition). Aging time: [day] for μAl, [hour] for nAl.

	Time [day], [hour]	Δm_0 [%]	$T_{onset,1}$ [K]	$\alpha_{Al\rightarrow Al_2O_3}$(933 K) [%]	$\alpha_{Al\rightarrow Al_2O_3}$ (1223 K) [%]
μAl-30	14	−4.3 ± 0.1	895.9 ± 0.6	0.6 ± 0.3	2.4 ± 0.6
μAl-7.5	14	−13.9 ± 0.2	884.3 ± 0.3	1.9 ± 0.6	8.6 ± 0.6
nAl-100	24	−2.1 ± 0.2	857.6 ± 0.5	37.5 ± 0.9	82.5 ± 1.5
	72	−32.1 ± 0.2	Not identifiable	10.0 ± 0.1	10.6 ± 0.1

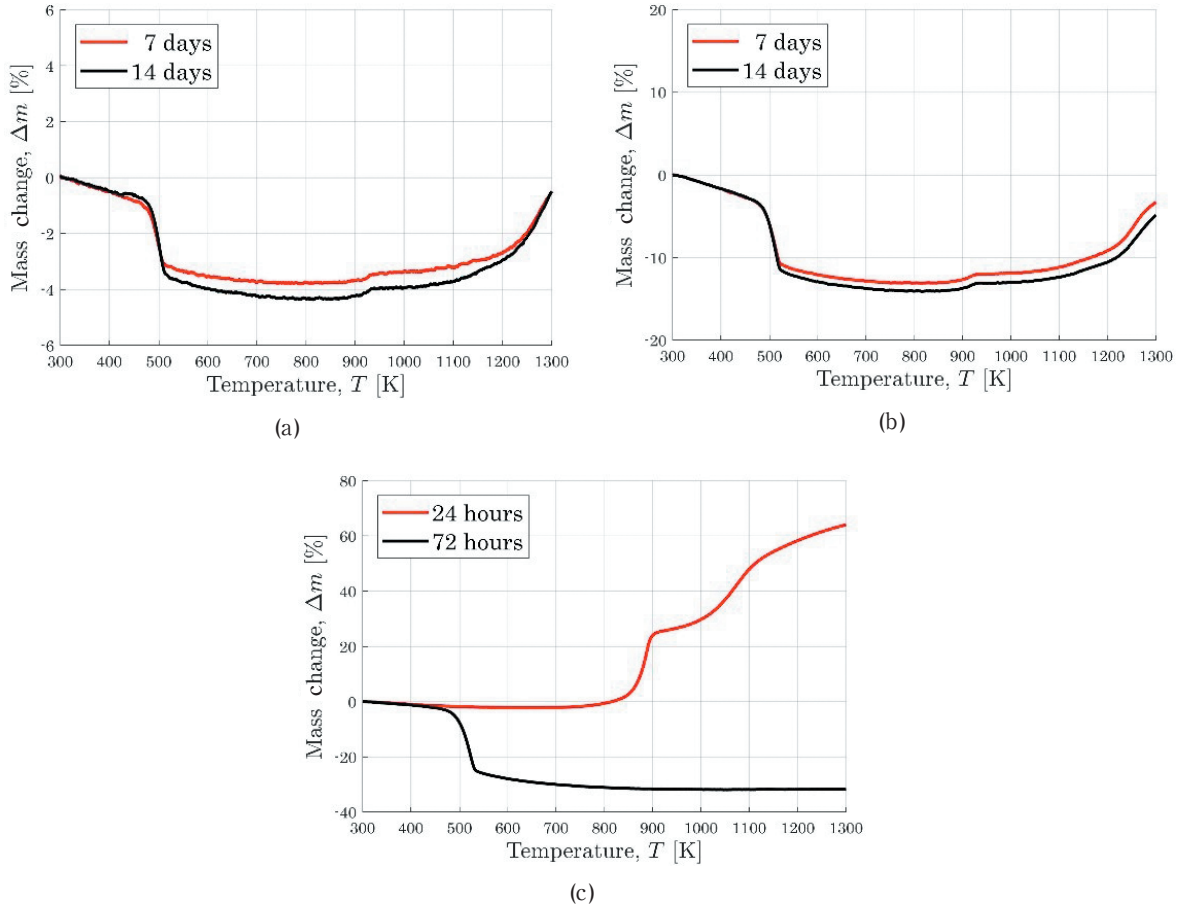

Figure 4 TG traces (air, 10 K min^{-1}, 0.1 MPa) of (a) μAl-30, (b) μAl-7.5 and (c) nAl-100, all under H1 condition.

sized powders. No significant aging effects are noticed for powders stored at 333 K with $RH < 10\%$ for 14 days (see Figure 2). Considering the storage under humid conditions (H1), differences are highlighted between micron- and nano-sized powders. Micron-sized powders show similar $C_{Al}(t)$ and $\alpha_{Al\rightarrow Al(OH)_3}(t)$, with a step decrease of the active metal content, and a corresponding increase in the $\alpha_{Al\rightarrow Al(OH)_3}$ after 7 days of storage (Figure 3). This suggests the existence of a threshold thickness for the hydrated species passivation action. For the tested μAl, this limiting thickness (calculated[1]) for C_{Al} (336 hours.), $Al(OH)_3$ density of 3080 kg m^{-3}, and the D_{32} values of the Table 1), is in the range 0.6–3.0 μm.The lower limit of this range exceeds the tested nAl size. The nAl-100 shows a weaker resistance to the humid environment. The powder C_{Al} decreases monotonically reaching limiting values of nearly 2 wt% in 72 hours. According to TG analyses and open literature data[14], the powder modifications are likely due to the formation of different aluminum hydroxide polymorphs (see Δm_0 and $T(\Delta m_0)$ in Table 3). The aging of the powders yields reduced $Al\rightarrow Al_2O_3$, conversion. Future developments of this work will focus on a deeper investigation of the thermal behavior of the aluminum powders for points of incipient change of the disperse system characteristics, and on an evaluation of the effects of higher heating rates on the thermal behavior of the materials.

Acknowledgement

This work is partially financed by the GRAIL H2020 program (EU grant agreement no. 638719). The authors thank Dr. Gianluigi Marra (ENI, Centro Ricerche per le Energie Rinnovabili e l'Ambiente) for the helpful discussions.

References

1) C. Paravan, F. Maggi, S. Dossi, G. Marra, G. Colombo, and L. Galfetti, "Energetic Nanomaterials", 341–368, Elsevier (2016).
2) L.T. DeLuca, L. Galfetti, F. Severini, L. Meda, G. Marra, A.B.

Vorozhtsov, V.B. Sedoi, and V.A. Babuk, Combust. Explos. Shock Waves, 41, 680–692 (2005).
3) L. Galfetti, L.T. DeLuca, F. Severini, G. Colombo, L. Meda, and G. Marra, Aerosp. Sci. Technol., 11, 26–32 (2007).
4) M.A. Trunov, M. Schoenitz, X. Zhu, and E.L. Dreizin, Combust. Flame, 140, 310–318 (2005).
5) A. Sossi, E. Duranti, M. Manzoni, C. Paravan, L.T. DeLuca, A.B. Vorozhtsov, M.I. Lerner, N.G. Rodkevich, A.A. Gromov, and N. Savin, Combust. Sci. Technol., 185, 17–36 (2013).
6) A. Sossi, E. Duranti, C. Paravan, L.T. DeLuca, A.B. Vorozhtsov, A.A. Gromov, Y.I. Pautova, M.I. Lerner, and N. G. Rodkevich, Appl. Surf. Sci., 271, 337–343 (2009).
7) M. Cliff, F. Tepper, and V. Lisetsky, AIAA Paper 2001-3287 (2001).
8) Y. Li, W. Song, C. Xie, D. Zeng, A. Wang, and M. Hu, Mater. Chem. Phys., 97, 127–131 (2006).
9) O.B. Nazarenko, Y.A. Amelkovich, and A.I. Sechin, Appl. Surf. Sci., 321, 475–480 (2014).
10) A.B. Vorozhtsov, L.T. DeLuca, A. Reina, M.I. Lerner, and N. G. Rodkevich, Sci. Tech. Energetic Materials, 76, 105–109 (2015).
11) S. Pisharath, F. Zhang, and H.G. Ang, Thermochim. Acta, 635, 59–69 (2016).
12) S. Cerri, M.A. Bohn, K. Menke, and L. Galfetti, Cent. Eur. J. Energ. Mater., 6, 149–165 (2009).
13) A.P. Ilyin, A.A. Gromov, V. An, F. Faubert, C. De Izarra, A. Espagnacq, and L. Brunet, Propellants Explos., Pyrotech., 27, 361–364 (2002).
14) T. Sato and J. Therm. Anal. Calorim., 32, 61–70 (1987).